Characterization of compressive properties of high-performance polymer fibres with a new microcompression apparatus

K. S. Macturk and R. K. Eby
The University of Akron, Department and Institute of Polymer Science, Akron, OH 44325-3909, USA

and W. W. Adams
Air Force Wright Research and Development Center, Dayton, OH 45433-6533, USA
(Received 10 August 1990; accepted 17 December 1990)

A microcompression apparatus to measure the compressive stress–strain curve of individual fibres has been developed. Illustrative results were obtained for a series of mesophase-pitch-based carbon fibres. A series of optical micrographs of a P100 fibre were taken as it failed in compression. The ultimate compressive strength (*UCS*) for any given type of fibre tended to cluster around two average values. The reason for this clustering is uncertain, but the two values may correspond to more and to less 'perfect' fibres. P55 exhibited a higher average *UCS* of 600 MPa and a lower average *UCS* of 300 MPa. P75 had a higher average *UCS* of 600 MPa and a lower average *UCS* of 300 MPa. P100 gave a higher average *UCS* of 400 MPa and a lower average *UCS* of 150 MPa. The compressive modulus for P75 was 470 GPa. The fibres exhibited non-linear elasticity, with the compressive modulus decreasing as the compressive strain increased.

(Keywords: fibre; compressibility; elasticity)

INTRODUCTION

Many high-performance polymeric fibres have been introduced for use as reinforcing elements in composites. These fibres have tensile strengths of the order of 1 GPa and elastic moduli of the order of hundreds of gigapascals. It is a somewhat lesser known fact that these fibres, with few exceptions, have compressive strengths that are 10–20% of their tensile strengths. The properties of fibres that are used as reinforcing elements in composites are very important since they provide the greater part of the strength and modulus of the composite. The relatively low compressive strength of the fibres is an important limitation on the use of composites in structural applications. Therefore, if it is desired to improve the structural properties of the composite, improving the compressive strength of the fibres is an obvious place to start.

There are several factors that have been investigated as the source of low fibre compressive strength. Some of these are: fibre buckling; microfibril buckling; glass transition temperature; fibre morphology and microstructure; as well as intermolecular interactions[1]. Factors that dominate compressive strength are very dependent on the particular type of fibre being examined. No hypothesis has been proven conclusively.

A serious impediment to investigating failure mechanisms in order to improve compressive strengths of the fibres is the lack of an accurate, reproducible method to obtain the compressive stress–strain curve for an individual fibre. There are several considerations that make this type of measurement difficult. The small diameter of the single fibres, approximately 10 μm, is the major obstacle. Sample preparation is time-consuming, options for holding the fibre are limited, and proper alignment of the fibre to avoid off-axis loading that induces buckling is difficult. Also, the apparatus performing the test must be capable of fine displacement control, fine force measurement and fine displacement measurement.

Several methods are available to measure the compressive strengths of individual fibres. Some examples include the bending beam test[2], the elastica loop method[3], single fibre in a matrix[4], the tensile recoil method[5], and the conversion of a micro-tensile testing machine to do compressive measurement[6]. Each has a unique set of operating conditions and can provide different information about the physical properties of the sample. The results obtained for compressive strength vary widely from one method to another (*Table 1*). No method is completely satisfactory, for various reasons. Some of these are complex stresses, analytical assumptions, the method of determining failure and a lack of sensitivity in stress and strain measurements.

EXPERIMENTAL METHOD

Three types of fibre were examined in this study. They were a series of mesophase-pitch-based graphite fibres (P55, P75, P100) made by Amoco. The number of samples of each type varied between seven and nine.

The experimental apparatus, which is mounted on an optical microscope stage, is shown in *Figure 1*. One end of a fibre sample is epoxied to a metal surface attached

Paper presented at Speciality Polymers '90, 8–10 August 1990, The Johns Hopkins University, Baltimore, MD, USA

0032-3861/91/101782-06

Table 1 Compressive strengths (MPa) obtained from various test methods

Fibre type	Elastica loop	Bending beam	Recoil method	Single fibre in matrix	Micro-tensilometer
P55			500[8]		
P75		1300–2000[7]	500[8]		
P100			400[8]		
Kevlar™	740–790[5]	620[7]	358[9]	850[4]	210[6]
PBO	680[5]	276[7]	193[9]	420[4]	300[6]
PBZT	680[5]	270[7]	276–413[9]	276[9]	

PBO = poly(p-phenylenebenzobisoxazole)
PBZT = poly(p-phenylenebenzobisthiazole)
Kevlar = poly(p-phenylene terephthalamide)

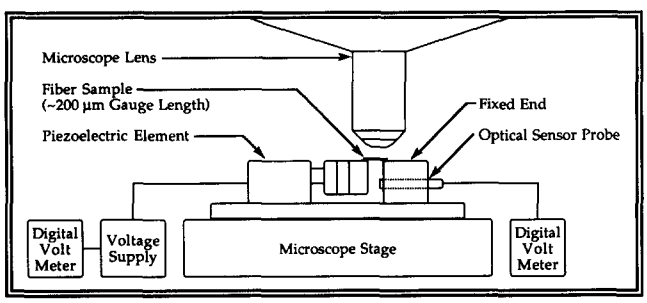

Figure 1 Schematic of experimental set-up

to a piezoelectric positioning element. The other end of the fibre is epoxied to a fixed metal surface. Fine grooves are located on the metal surfaces supporting the fibre parallel to the crystal axis in order to aid fibre alignment. Proper alignment of the fibre is necessary to avoid buckling. Before a measurement begins, the gauge length and diameter of the sample are measured with the optical microscope. The gauge length is defined as the length of fibre between the points where epoxy covers the fibre on each end.

The test begins by applying a voltage to the piezoelectric element, causing it to expand and place the fibre in compression. The displacement of the piezoelectric element is measured by an optical probe[10]. The voltage applied and corresponding displacement are recorded. The test continues until the engineering compressive stress, which can be calculated from an equation given below, has dropped to almost zero. After the test is complete, the fibre sample is examined with the optical microscope and the presence and orientation of any cracks in the fibre are noted.

The equation used to obtain the force exerted by the piezoelectric element is as follows[11]:

$$F = S\,\mathrm{d}l - dV \tag{1}$$

where F is the force exerted by the crystal, S the stiffness of the crystal, $\mathrm{d}l$ the displacement of the crystal, d the piezoelectric constant relating force and voltage, and V the voltage applied to the crystal. Thus, if the material constants (S and d), the displacement of the crystal and the voltage applied are known, the force can be calculated. By measuring the gauge length and diameter of the specimen before a test, one can produce a stress–strain curve.

EXPERIMENTAL CONSIDERATIONS

Compliance corrections

There are two other important considerations. The first is test fixture compliance. Since the displacements of the fibre are on the submicrometre scale, any displacement of the fixture will be significant relative to the crystal displacement and must be taken into account. When the test fixture compliance is considered, the force equation appears as follows:

$$F = (S\,\mathrm{d}l - dV)/[1 - S(1/k_1 + 1/k_3)] \tag{2}$$

where k_i is the stiffness of the test fixture. There are two stiffness values because it was found during the measurement of the test fixture stiffness that each end of the fixture displaced slightly. These were analysed in terms of two different stiffness values. They could, of course, be represented by one overall stiffness.

The second consideration is the compliance of the epoxy. When a force is applied, the result is a deformation not only of the fibre, but also of the epoxy. This will not introduce error into the calculation of the force applied to the fibre, but it will introduce error into the apparent strain in the fibre. Thus, values for the modulus and the strain to failure require a correction for the epoxy compliance.

A value for the compliance of the epoxy was obtained in the following manner. The average apparent compliance values at small strains for two types of fibre were computed from measurements without any correction for the epoxy compliance. Values for the stiffness of each of the types of fibre at small strains in tension were also obtained from the literature[12]. The stiffness values at very small strains in tension were set equal to the stiffness values at small strains in compression.

For strains up to 0.05%, a graph of measured fibre compliance *versus* fibre compliance derived from the tensile stiffness was produced (*Figure 2*). A line was fitted to the measured compliance for the P55 and P100 fibres. The differences between this line and the literature tensile values mentioned above were taken as the corrections for the epoxy compliance. The correction was obtained for the P75 fibre. This epoxy compliance was subtracted from the measured value to obtain the corrected fibre compliance. Using the latter, together with the average area and gauge lengths of the samples, yielded a modulus for P75.

Sample length effects

Euler developed the relationship between geometry,

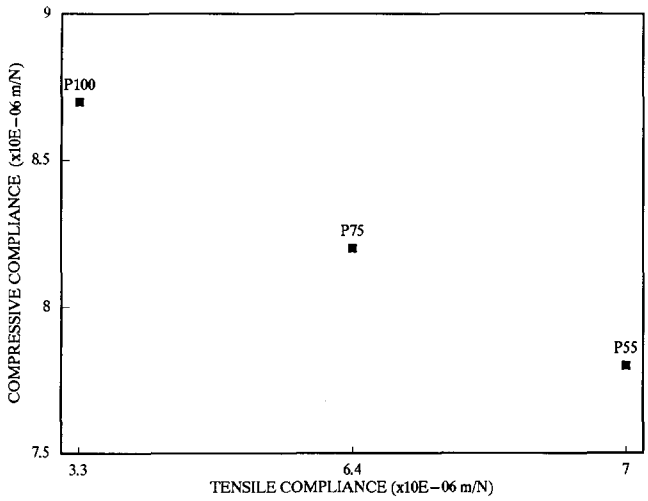

Figure 2 Graph of measured compressive compliance *versus* tensile compliance at small strains

elastic properties and compressive failure by buckling. Euler's equation, for the case of rigidly clamped ends, is as follows:

$$P_{cr} = 4\pi^2 EI/L^2 \quad (3)$$

where P_{cr} is the critical load to induce buckling, E the tensile modulus, L the length of the sample, I the area moment of inertia of the specimen, and $\pi = 3.14\ldots$. The moment of inertia for a column is $I = \pi r^4/4$, where r is the radius of the column. It can be seen from equation (3) that buckling is dominated by geometry, and therefore gives little useful information about the strength of a material.

An estimate of the maximum fibre length that can be used without failure by buckling (L) can be estimated by substituting for I in equation (3), converting the critical load to a critical stress, $\sigma_{cr} = P_{cr}/\pi r^2$, and solving for L. Substituting values from the literature for E ($E_{P55} = 305$, $E_{P75} = 450$ and $E_{P100} = 770$ GPa[13]), σ_{cr} ($\sigma_{P55} = 500$, $\sigma_{P75} = 500$ and $\sigma_{P100} = 400$ MPa[8]) and the fibre radius of 5 μm yields approximate maximum lengths to avoid buckling of $L_{P55} \approx 400$, $L_{P75} \approx 500$ and $L_{P100} \approx 700$ μm. Using gauge lengths that are slightly shorter than these values will not entirely ensure the absence of failure by buckling, however. Instead, failure will occur by a combination of buckling and pure compression[14].

Pure compressive failure is achieved only in columns that have a length equal to or less than 10 times the least lateral dimension of the column[14]. Since the diameter of the fibres tested was approximately 10 μm, a gauge length of 100 μm is needed to avoid Euler buckling. It is only in this region that the compressive stress at failure reflects a material property and the well known Hooke's law may be used[14].

Another consideration that limits sample geometry is the non-uniform stress distribution introduced by clamping. For transversely isotropic materials, such as many high-performance fibres, the decay length for uniform stress over the cross-section, defined as δ, is given by[15]:

$$\delta = r(E/E_t)^{1/2} \quad (4)$$

where E_t is the transverse modulus of the specimen. Once again, by using values in the literature, estimates of the decay length can be found: for P55, $E_t = 10.8$ GPa[13], thus $\delta_{P55} \approx 30$ μm; for P75, $E_t = 8.8$ GPa[13], so $\delta_{P75} \approx 40$ μm; for P100, $E_t = 7.1$ GPa[13], so $\delta_{P100} \approx 50$ μm. These are the minimum lengths away from the end of the sample necessary to allow the stress distribution across the cross-section of the column to become reasonably uniform. Doubling these values to account for both ends of the fibre gives a minimum gauge length l necessary to reduce end effects. Thus, $l_{P55} \approx 60$ μm, $l_{P75} \approx 80$ μm and $l_{P100} \approx 100$ μm. In reality, it is desirable to have minimum gauge lengths that are larger in order to reduce even further the end effects arising from clamping.

In theory then, the samples for each fibre type used in this study should have gauge lengths between the minimum length allowable to avoid end effects, l, and the maximum length allowable to avoid Euler buckling, L. In addition, it is desirable to have the maximum length as close to $20r$ as possible to ensure failure in pure compression. These three requirements oppose one another and the effects arising from all three need to be minimized simultaneously. This can be done most efficiently by increasing the radius of the fibre. The samples used in this study had an average gauge length of approximately 200 μm and an average radius of 5 μm.

RESULTS AND DISCUSSION

A representative engineering stress–strain curve for P75 is shown in *Figure 3*. It is interesting to note that this sample exhibits non-linear elasticity. The relationship between compressive stress and strain appears to be non-linear, with the slope decreasing with increasing compressive strain. This was true for all three types of fibre tested.

The ultimate compressive strength (*UCS*) results obtained from such curves are summarized in *Table 2*. Each type of fibre gave results that tended to cluster around a higher and a lower *UCS* value. The F test[16] showed that the higher and lower averages had a high

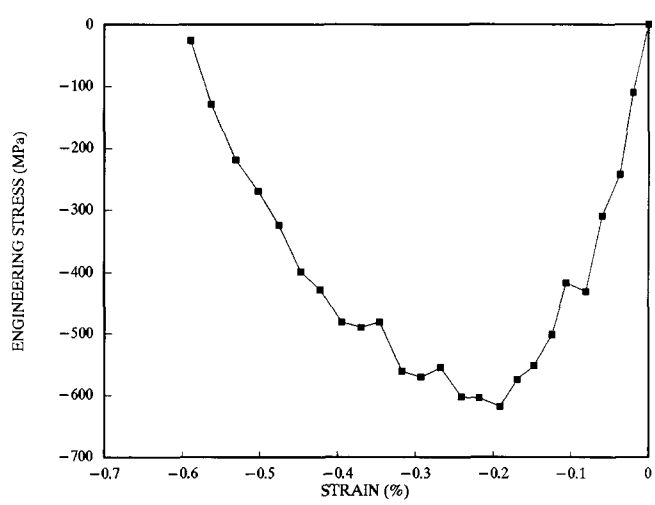

Figure 3 Representative engineering stress–strain curve for P75

Table 2 Ultimate compressive strength (MPa) results from this study

Fibre type	Overall average	Higher average	Lower average
P55	400	600	300
P75	400	600	300
P100	200	400	150

probability of being different. Therefore, both values as well as an overall average are reported here. P55 gave an overall average *UCS* of 400 MPa with a standard deviation of 150 MPa. The higher average *UCS* was 600 MPa and the lower average *UCS* was 300 MPa. The results for P75 were an overall average *UCS* of 400 MPa with a standard deviation of 150 MPa, while the higher average *UCS* was 600 MPa and the lower average *UCS* was 300 MPa. The compressive modulus was 470 GPa. Finally, P100 gave an average *UCS* of 200 MPa with a standard deviation of 150 MPa. The higher average *UCS* was 400 MPa and the lower average *UCS* was 150 MPa.

Table 3 Comparison of results for *UCS* (MPa) from the recoil method[8] and the microcompression apparatus

Fibre type	Recoil method	Microcompression apparatus (average)
P55	500	400
P75	500	400
P100	400	200

The mechanisms behind the grouping of the *UCS* values are unknown. It is possible that the lower values result from the presence of defects in the fibre. These defects could be inherent in the fibres themselves or may result from handling and preparation of the fibre samples. If the former is the case, the higher average may be thought of as the 'ideal' fibre *UCS* and the lower average as dominated by flaws or damage in the samples. However, one cannot presently rule out the possibility of experimental errors such as slight fibre misalignment contributing to this effect.

The average compressive strengths obtained in this

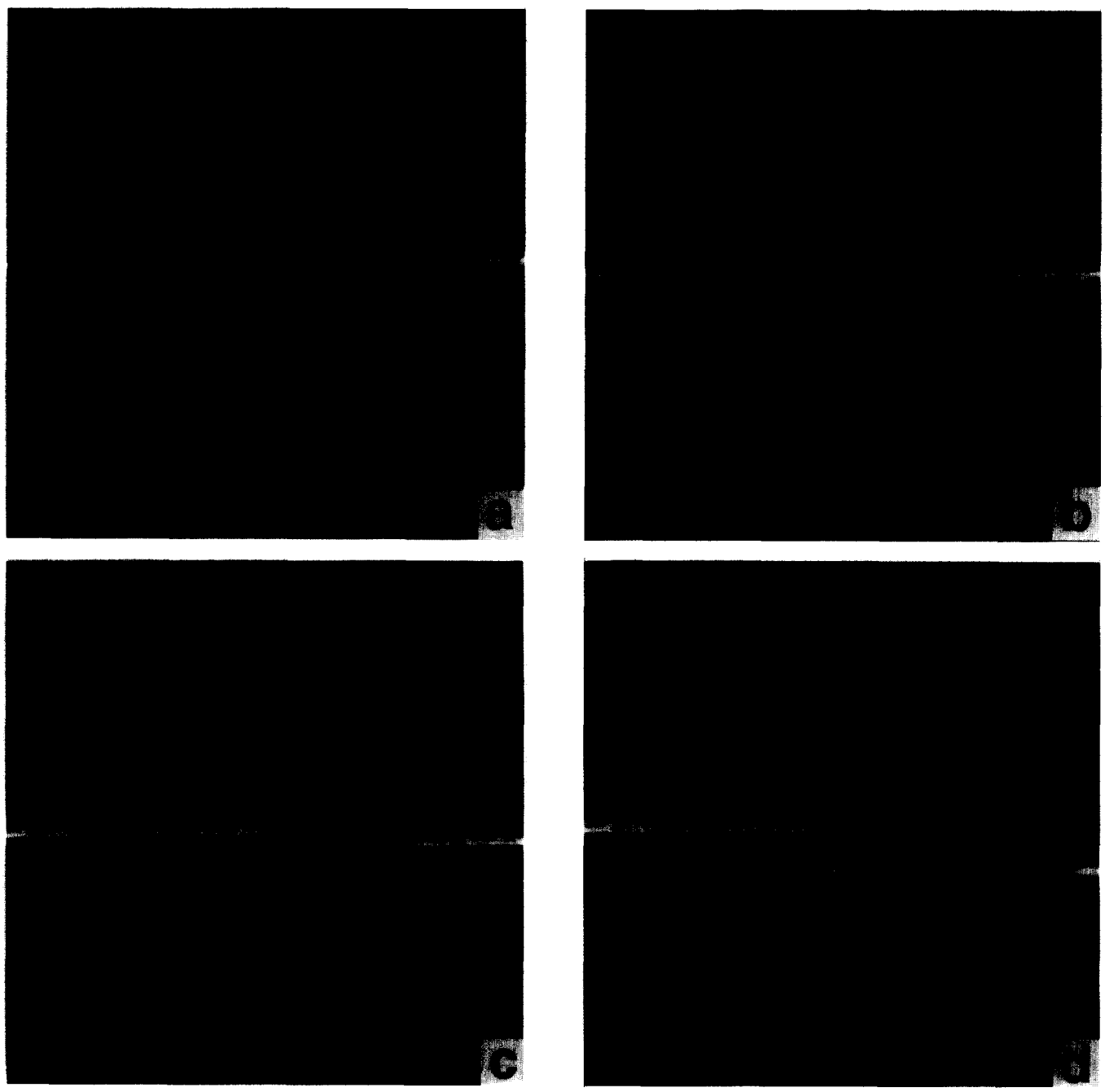

Figure 4 Optical micrographs of a P100 fibre with various voltages applied to the piezoelectric driver: (a) 0 V; (b) −30 V; (c) −75 V; (d) −210 V

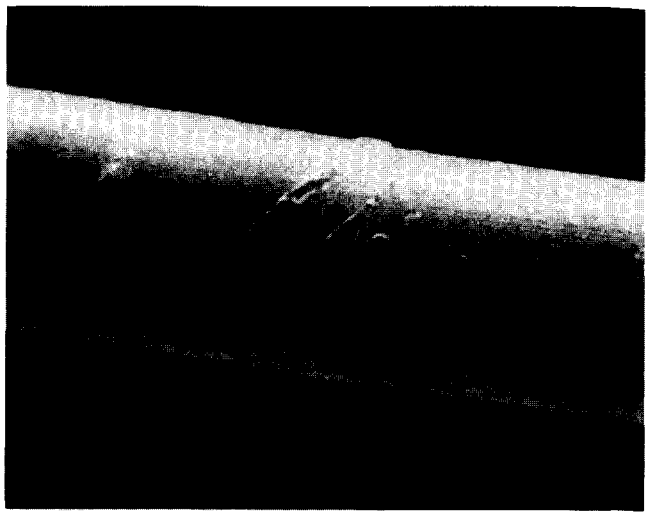

Figure 5 Scanning electron micrograph of a P100 fibre in early stages of failure. The fibre diameter is 10 μm

study are similar to those obtained by the recoil method[8]. In particular, the results for the overall average *UCS* of all the fibres were slightly lower than the values obtained by the recoil method (*Table 3*). The upper cluster values were higher and the lower cluster values lower than the recoil results.

A series of optical micrographs were taken of a P100 fibre as it failed in compression. These micrographs were taken after a test, since use of the light microscope affected operation of the optical probe. Thus, the voltage applied to the piezoelectric element is given instead of either the stress or the strain. Increasing negative voltage applied to the piezoelectric element corresponds to increasing compressive strain in the fibre. The first (*Figure 4a*) shows the fibre with no voltage applied to the piezoelectric crystal. The second (*Figure 4b*) is with -30 V applied. This is past the point of failure in the stress–strain curve and a region of deformation that appears planar is now visible. The normal to the plane is at about 25° to the fibre axis. The third micrograph (*Figure 4c*) is with -75 V applied. Some material can be seen between the two ends of the fibre. The fourth (*Figure 4d*) micrograph is with -210 V applied. The two ends of the fibre are now clear of each other.

Preliminary work was also done using the apparatus in an SEM. Resulting micrographs taken at an early stage in the fracture process revealed multiple regions of deformation in the fibre (*Figure 5*). These preliminary results show that the microcompression apparatus may be used in the SEM to study the mechanism of the fracture in real time. It also means the process can be monitored at lower stresses in real time, when the failure is just beginning and not yet visible optically.

One major advantage of this apparatus is that it provides a stress–strain curve. Another advantage is that failure is detected in an objective manner from the shape of a stress–strain curve. In contrast with other methods, visual observation of failure is not necessary. This means that the point of failure can be detected in a more sensitive manner, before the large amount of damage that is needed to determine failure visually has accumulated in the fibre. Finally, the compression failure process can be studied using X-ray diffraction as well as optical and electron microscopy.

There are a number of sources of variation in the results obtained from this study. The first is the fibre itself. As is the case with tensile strength[17], the compressive strength for an individual fibre might be expected to vary greatly from one fibre to the next. In addition, the handling of the sample during preparation and mounting may produce flaws, which will affect the results. A second possible source of error is incorrect alignment of the sample. A light microscope (500 ×) was used to align the fibre prior to a test. The inability to use higher magnifications during the alignment process may result in some small misalignment of the sample. Thirdly, the method of securing the fibre in place may be a source of error. In this study, the integrity of the bond between the epoxy and the fibre was paramount. Anything less than a 'perfect' bond would allow the fibre to slip, resulting in incorrect strain readings. This might have been the largest source of error.

There are two steps that could be taken to improve the method. The first is to find a better way to secure the fibre in place. The difficulty in rigidly holding a fibre that has a diameter of 10 μm should not be underestimated. Another improvement would be to use separate piezoelectric elements to displace the fibre and measure the force. This would allow for more sensitive force measurement and finer displacement control.

SUMMARY AND CONCLUSIONS

A new method to measure the compressive stress–strain curves of individual high-performance polymeric fibres has been developed. Three types of carbon fibres produced by Amoco from mesophase pitch were tested. The results compared rather well with results from the recoil method. The overall average *UCS* for both P55 and P75 was 400 MPa. In addition, the higher average *UCS* was 600 MPa and the lower average *UCS* was 300 MPa. For P100 the overall average *UCS* was 200 MPa with a higher average *UCS* of 400 MPa and a lower average *UCS* of 150 MPa. The higher strength values may be associated with relatively more perfect fibres and the lower values with fibres where failure is dominated by flaws and damage from handling. A compressive modulus of 470 GPa was obtained for P75. The relationship between stress and strain appears to decrease with increasing compressive strain, indicating the presence of non-linear elasticity.

This apparatus has advantages over other methods in use. First, a stress–strain curve is obtained for the fibre in compression, allowing failure determination to be made objectively. This allows for more accurate determination of the ultimate compressive strength of the sample. In addition, both the *UCS* and the compressive modulus of a fibre can be measured.

There are other potential applications of this apparatus to allow more extensive characterization of high-performance fibres. The first is that optical and scanning electron microscopy may be used for real-time examination of the fibre sample during the test and to provide correlation between the failure process and the stress in the fibre. A second potential application would be using X-rays or birefringence measurements to examine how the microstructure of the fibre changes as it undergoes compression. It is expected that better correlation between the microstructure of the fibre and its macro-

scopic compressive properties will lead to high-performance fibres with improved compressive properties.

ACKNOWLEDGEMENTS

This work was supported by the Air Force Office of Scientific Research (AFOSR-87-0320), the Wright Materials Laboratory Director's Fund and the Johns Hopkins Center for Nondestructive Evaluation. The experimental work was performed while the first two authors were at the Johns Hopkins University.

REFERENCES

1 Kumar, S. and Helminiak, T. E. in 'Materials Research Society Symposium Proceedings' (Eds W. W. Adams, R. K. Eby and D. E. McLemore), Pittsburgh, PA, 1989, Vol. 134, p. 363
2 DeTeresa, S. J. 'The Axial Compressive Strength of High Performance Fibers', AFWAL-TR-85-4013, 1985
3 Sinclair, D. *J. Appl. Phys.* 1950, **21**, 380
4 Drzal, L. T. 'The Interfacial and Compressive Properties of High Performance Polymeric Fibers', AFWAL-TR-86-4003, 1986; see also Hawthorne, H. M. and Teghtsoonian, E. *J. Mater. Sci.* 1975, **10**, 41
5 Allen, S. R. *J. Mater. Sci.* 1987, **22**, 853
6 Fawaz, S. A. 'Compressive Properties of High Performance Fibers', AFWAL-TR-88-4262, 1989
7 DeTeresa, S. J., Porter, R. S. and Farris, R. J. *J. Mater. Sci.* 1988, **23**, 1186
8 Dobb, M. G., Johnson, D. J. and Park, C. R. *J. Mater. Sci.* 1990, **25**, 829
9 Wang, C. S., Bai, S. J. and Rice, B. P. *Proc. ACS Div. Polym. Mater. Sci. Eng.* 1989, **61**, 550
10 Cook, R. O. and Hamm, C. W. *Appl. Opt.* 1979, **18**, 3230
11 Mason, W. P. 'Piezoelectric Crystals and Their Application to Ultrasonics', Van Nostrand, New York, 1950
12 Arsenovic, P., Jiang, H. *et al.* in 'Carbon '88' (Eds. B. McEnaney and T. J. Mays), IOP Publishing, Bristol, 1988, p. 487
13 Wagoner, G., Smith, R. E. and Bacon, R. in 'Proceedings and Program, 28th Biennial Carbon Conference', American Carbon Society, 1987, p. 416
14 Pytel, A. and Singer, F. L. 'Strength of Materials', Harper and Row, New York, 1987, pp. 387–405
15 Horgan, C. O. *Int. J. Solids Struct.* 1974, **10**, 837
16 Bevington, P. R. 'Data Reduction and Error Analysis for the Physical Sciences', McGraw-Hill, New York, 1969, p. 200
17 Moreton, R. in 'Handbook of Composites' (Eds A. Kelley and Y. N. Rabotnov), Elsevier, New York, 1985, Vol. 1, p. 469